非定常空力現象兆候検出へのデータマイニング試行

A first attempt for detecting transonic buffet signature via unsteady-data mining

By Kazuhisa CHIBA,[1)] Shinya WATANABE,[2)] Masaya NAKATA,[3)] Yuhei UMEDA,[4)] Naoki HAMADA,[4)] Kanako YASUE,[5)] Koji SUZUKI,[5)] Shigeru KUCHI-ISHI,[5)] Kazuyuki NAKAKITA,[5)] and Takeshi ITO[5)]

[1)] *The University of Electro-Communications, Tokyo, Japan*
[2)] *Muroran Institute of Technology, Hokkaido, Japan*
[3)] *Yokohama National University, Yokohama, Japan*
[4)] *Fujitsu Laboratories Ltd, Kawasaki, Japan*
[5)] *Japan Aerospace Exploration Agency, Tokyo, Japan*

The transonic buffet degrades the aerodynamic performance of the aircraft during cruise. It is a phenomenon that should be avoided absolutely as it may lead to accidents. However, the mechanism of occurrence has yet to be elucidated. To understand this phenomenon, large-scale unsteady data is accumulated using computational fluid dynamics. In contrast, data mining of time series data such as unsteady data is a recent topic in that field. In this study, we have attempted to perform unsteady data mining with capacity exceeding Tera's order. As a result, the behavior of the physical quantity before the transonic buffet arises was suggested to be different from the data just before the transonic buffet occurs. Moreover, a topological data analysis revealed abnormalities before the temporal origination determined by visualizing flow structure. Based on the results, we visualized the data over time, and found the characteristic change of the viscosity distribution on the wing surface. This should be a clue to elucidate this phenomenon.

Key Words: Data mining, Unsteady aerodynamic data, Transonic buffet, Sign detection, Airplane

1. Introduction

Unfortunately, the current civil aircraft has transonic cruises because the supersonic aircraft Concorde has retired. Because the shockwave interacts with the separated boundary layer, many transient phenomena occur under transonic flow conditions. The resulting pressure fluctuations cause a number of undesirable unstable effects and therefore there is the possibility of shockwave oscillations known as transonic buffets on the wing surface of the airplane [1)].

This is a phenomenon in which the interaction between the shockwave and the turbulent boundary layer and the separation of the flow cause a large self-sustained fluctuation on the profile at the transonic Mach number. Shock-induced variations often lead to periodic impact motion with large amplitude at high subsonic Mach numbers. Although these shockwave movements were reported in 1947 [2)], the physical mechanism of the wing transonic buffet is still unknown despite the possibility of inducing a severe accident. So the transonic buffet is one of the most important topics in the experimental / computational aerodynamic field. When transonic buffet occurs in a civil aircraft sailing on a daily basis, it is an extremely dangerous phenomenon due to falling into a stall and therefore has a flight profile such that a transonic buffet never occurs. Elucidation of the cause is a matter of great urgency.

Past experiments and calculations show that the transonic buffet phenomenon is low frequency oscillation [3)]. It is slower on the order of $O(10^{-1})$ to $O(10^{-2})$ than the flow phenomena generated around the wing of the airplane. In recent years, experiments and calculations gradually capture the transonic buffet [4)], but its data is enormous in Tera-order due to the fine time scale. Because this is an acceptable quantity as one of Big data [5)], it is not possible to easily analyze data for the transonic buffet data set. Big data analysis is a topic in the field of data mining and extensive data analysis, however, in the field of aerospace engineering, it has not been able to successfully use time series data sets such as unsteady aerodynamic data. To acquire knowledge to make use of the design, it is necessary to obtain design information through data mining by effectively using accumulated unsteady data.

The ultimate goal of this project is to reveal the cause of the transonic buffet and to design a new geometry of the airplane wing or a device that does not produce transonic buffet on the aircraft. As a first step, this study determines the temporal and spatial origination of the transonic buffet temporally and spatially with respect to a time series data set with a transient phenomenon of transonic buffets constructed by Computational Fluid Dynamics (CFD). To do so, we tried several data mining techniques from conventional to state-of-the-art methods and examined the policy of the next step.

2. Numerical Methods

2.1. CFD

Unstructured detached eddy simulation (DES) is executed using FaSTAR (FaST Aerodynamic Routines) [6)] developed by Japan Aerospace Exploration Agency (JAXA). Summarize the calculation scheme for analyzing the transonic buffet by FaSTAR shown in Table 1.

We prepare a calculation model for NACA0012. The 3D model has a length of non-dimensional spanwise length of 0.5 under the dimensionless chord length of 1.0 shown in Fig. 1. We calculate under the Mach number $M = 0.72$ =const. For data mining, we obtain the data set from DES analysis with swept angle of attack (AoA) (linear angle of attack α sweep from 3.6 to 4.6 [deg] because the transient buffet is predicted from DES

Table 1. Computational schemes on FaSTAR for analyzing transonic buffet.

Governing equation	Full Navier-Stokes
Discretization	Cell-center
Mesh type	Structured
Inviscid flux	Harten-Lax-van Leer-Einfeldt-Wada [7]
Viscous flux	Cell gradient
Gradient evaluation	Weighted Green-Gauss
Limiter	Hishida's limiter
Turbulent model	Spalart-Allmaras (SA-no ft_2-R) [8]
Time integration	Lower/Upper-Symmetric Gauss Seidel [9]
Domain decomposition	METIS
Parallel computation	MPI

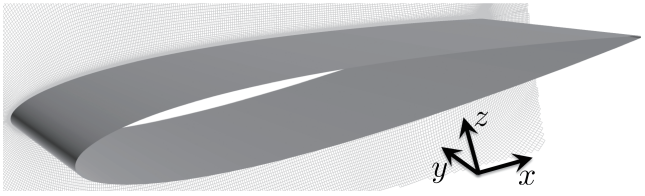

Fig. 1. Computational model using NACA0012. Generated meshes size are $501 \times 101 \times 161$.

analysis with fixed AoA near α of 4.1 [deg]). The initial value of DES analysis with swept AoA uses the result of DES with fixed AoA and starts continuation calculation. The dimensionless time step is 0.005 (roughly equivalent to real time 0.003 [s]) and 320000 steps are totally computed. $y = 0$ and $y = 0.5$ have periodic boundary condition. We acquire six output data: density ρ, x-directional velocity u, y-directional velocity v, z-directional velocity w, pressure p, and the turbulent eddy viscosity coefficient near the wall $\tilde{\nu}$.

Since the amount of data becomes enormous when physical quantities are acquired in all cells of the mesh, this time we create data sets for data mining at 60 monitoring points. The monitoring points #1 to #30 are on the top side surface of the computational model, and #31 to #60 are set as one layer upper mesh. In this paper, we will focus on the monitoring points from #1 to #30 due to similar tendencies. The monitoring points from #1 to #30 are shown in Fig. 2. The monitoring points from #1 to #10 are on $y = 0.10$, from #11 to #20 are on $y = 0.25$, and from #21 to #30 are on $y = 0.40$. The x coordinates of #1, #11, and #21 are set at $x = 0.05$, #10, #20, and #30 are set at $x = 0.50$. Other monitoring points are set at even intervals.

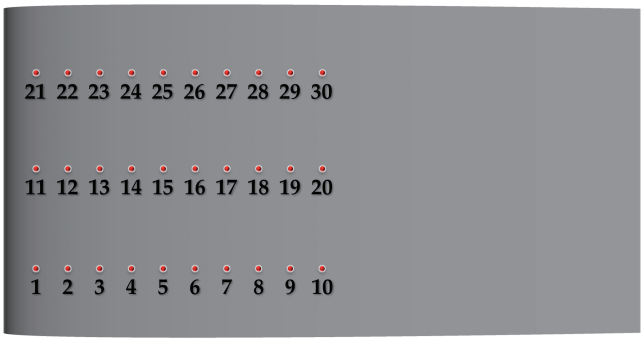

Fig. 2. The monitoring points on the upper surface of NACA0012 computational model.

2.2. Data Mining

We employ several data mining techniques: on-demand type correlation-based hierarchical structuring method (CIHSM) [10] including a parallel coordinate plots (PCP) [11] and a scatter plot matrix (SPM) [12], the Barnes-Hut-SNE (Stochastic Neighbor Embedding) [13], and the Betti sequence [14]. CIHSM is a type of rule mining, structuring generated rule set and clarifying the organic relationship between the rules. Each rule set applies PCP and SPM to examine a physical background which rule sets generate. PCP and SPM are the well-known general-purpose tool for multi-dimensional data visualization. Even though many visualization techniques have been supposed, PCP and SPM are still the simplest and the easiest to observe complex relationships among variables of high-dimensional data. The Barnes-Hut-SNE is an embedding technique that is commonly used for the visualization of high-dimensional data in SPM and that normally runs in $O(N^2)$.

In contrast, the Betti sequence analysis is based on the chaos theory [15] and the persistent homology [16]; it is one of the topological data analysis (TDA) [17] manners. The Betti sequence is the vector which describes the feature of attractor. It represents the following time evolution equation relative to time series using persistent homology:

$$x_{k+1} = f(x_k,\ x_{k-1},\ \cdots,\ x_1), \tag{1}$$

where x_i ($\forall x_i \in \Re$) denotes time series observations. We analyze the classification scores to cognize the occurrence of buffet via applying the above Betti sequence to unsteady aerodynamic data as TDA viewpoints. The detailed descriptions of the Betti sequence can be referred in [14].

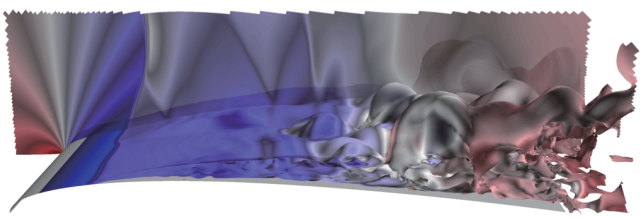

Fig. 3. Instantaneous situation of the CFD result in the transonic buffet on the wing upper region. We illustrate the wing upper surface, iso-surface of turbulent viscosity with C_p distribution, and the surface at $y = 0.40$ with C_p distribution.

3. Results

3.1. CFD Result as a Data Mining Dataset

CFD analysis is implemented in JSS2 (JAXA supercomputer system second generation). DES analysis with swept AoA takes about two weeks. In this calculation, *alpha* is shifted from 3.60 to 4.60 [deg]. This is because it was confirmed that the transonic buffet starts from approximately 4.12 [deg] in the result of the DES with fixed AoA separately performed (for effective parametric calculation of 2 decimal places, the effective digits are up to 2 decimal places). Analysis of the results obtained from DES analysis with swept AoA showed that the transonic region of transonic buffet is roughly 13% to 24% of the chord length; the Strouhal number S_t on the time scale based on the chord length ($S_t \approx 1$) is approximately 0.073 to 0.081. Thereupon, the current transonic buffet is a low frequent phenomenon.

Figure 3 shows the 3D flow of the instantaneous situation after the transonic buffet began to occur. It consists of an isosurface of the turbulent viscosity with a contour of the pressure coefficient C_p and a calculated surface with $y = 0.40$ with C_p contour. From this figure, we can know the flow structure under transonic buffet condition. Separation occurs behind the shockwave surface. The boundary layer grows, the transition region appears, and the turbulent boundary layer develops. We can also observe three-dimensional nonlinear structure.

3.2. Data-Mining Result

3.2.1. Result from PCP

The data of DES with swept AoA was analyzed from the following viewpoint:

- We compare six physical quantities' changes at whole monitoring points to find differences in trends by points.
- We analyze based on two viewpoints:
  - physical amounts themselves at each monitoring point at present time
  - difference of physical quantities between the immediately preceding and present time at each monitoring point

  to cognize the difference between that two viewpoints.
- We compare not only the values at each monitoring point but also the data of the surrounding spots with the values of the averaged data so that we analyze what kind of trend difference will occur.

Figure 4 shows the PCP results between well before and just before buffet occurs. As a consequence, the tendency greatly depends on the monitoring points; it was found that the closer to the shockwave, the more clearly the tendency is exhibited. Although it was confirmed that the trend greatly differs with the difference and the value itself, there was no large difference between the two in the strength of the trend.

Moreover, there is a part where the tendency is strengthened by taking the average of the surrounding monitoring points. The representative monitoring point is #5; we shows the PCP of the six physical quantities between the time before occurring transonic buffet and that immediately before occurring it. This figure simply explains the different tendency of the behavior of whole physical quantities, hence we will visualize the flow structure under the condition addressed by PCP in Chapter **4.** to clarify the physical reason of the different tendency.

3.2.2. Result from Barnes-Hut-SNE

Figure 5 illustrates the results of applying the Barnes-Hut-SNE at from #01 to #05. The five-dimensional physical quantity is expressed as a feature that is dimensionally compressed well than expected. Since the periodic and gradual changes of the physical quantities are drawn, this algorithm can also visualize the time series changes of the physical quantities. If we classify the physical quantity and examine the trend change, it may be applicable to sign detection. However, although there seems to be features, it is still unknown which physical quantity to focus on. Many of the dimensionally compressed features overlap and there are monitoring points that are difficult to grasp the features qualitatively but because we can not conclude that there is no physical quantity feature, we will consider coupling with other dimensional compression methods.

3.2.3. Result from the Betti Sequence

From the analysis results at all monitoring points, the results of #01 to #05 are shown as a representative example in Fig. 6. According to the CFD result, since the position in the chordwise direction is 13 to 24% in the oscillation region of the transonic buffet, the monitoring points #01 and #02 are always located in

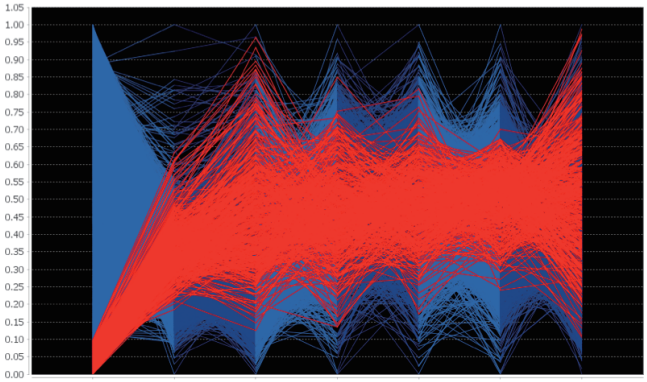

(a)

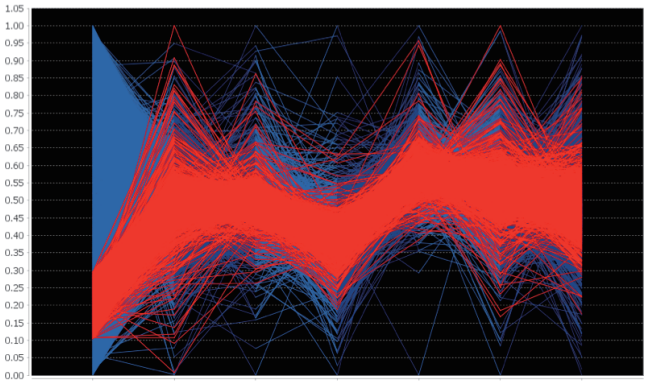

(b)

Fig. 4. PCP of averaged sampling difference. Red lines represent the data with conditional correspondence and blue lines denote other whole data. (a) the data at the time before occurring transonic buffet. (b) the data at the time immediately before occurring transonic buffet. Note that n_{itr} denotes the computational iteration number.

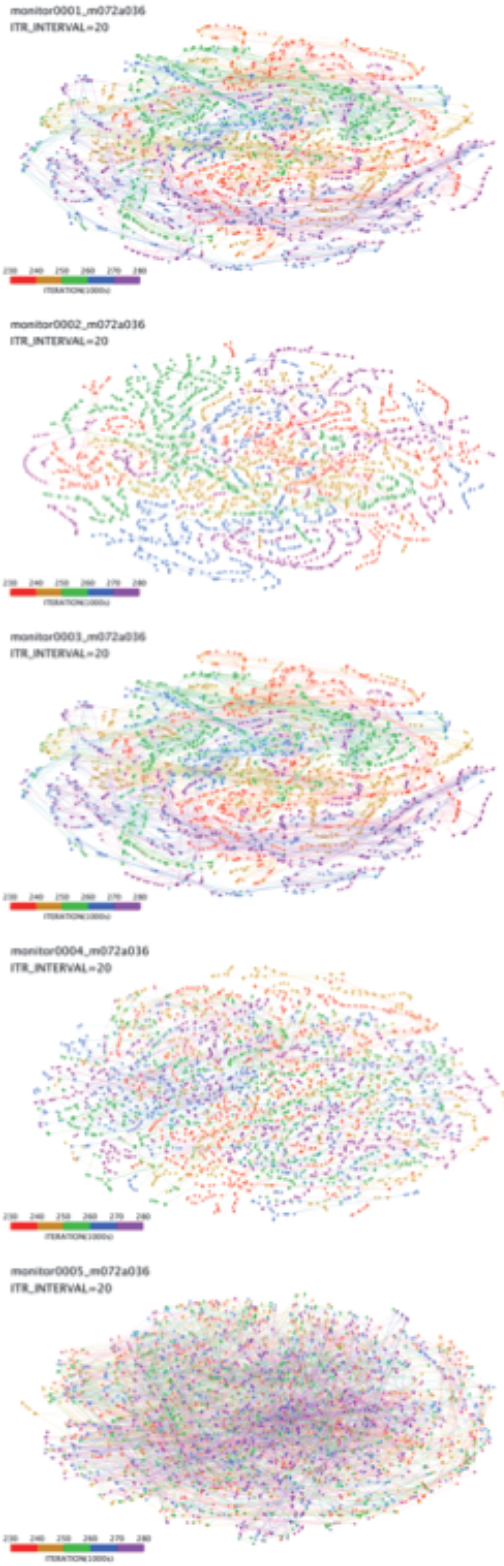

Fig. 5. The result of applying the Barnes-Hut-SNE at the monitoring points from #01 to #05.

front of the shockwave regardless of the time. Also, the monitoring points #03 and #04 are in shockwave oscillation, the point #05 always lies behind the shockwave regardless of the passage of time.

For monitoring points #01 and #02, the normal u is a constant value; the Betti sequence value is not detected. In contrast, time

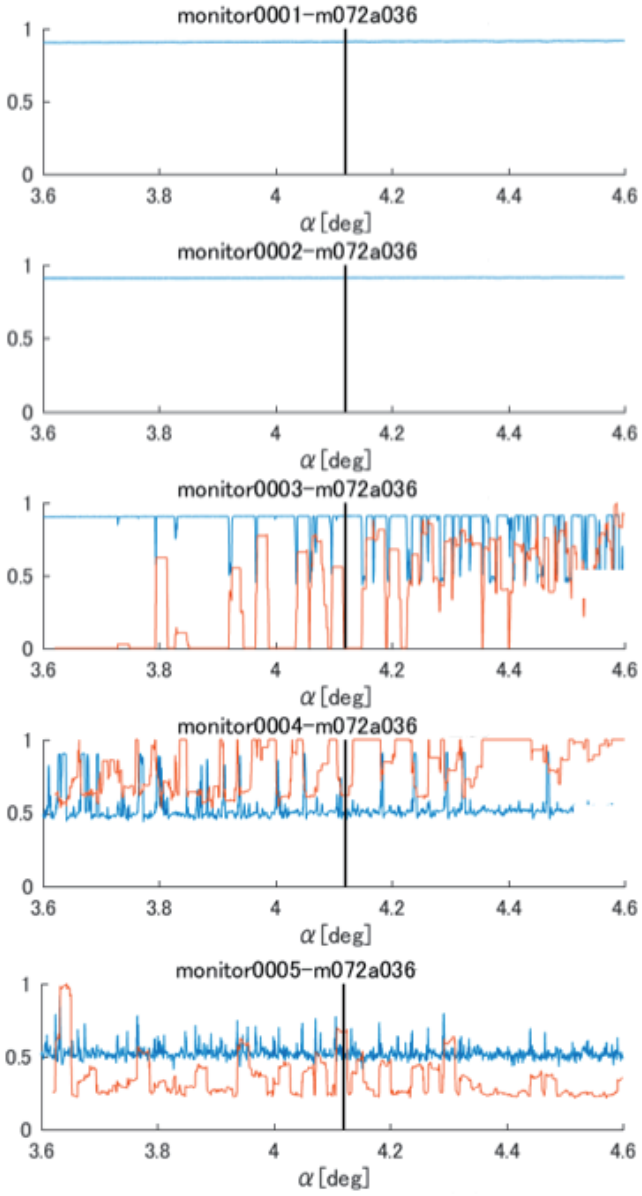

Fig. 6. The result of applying the Betti sequence to u physical quantity at the monitoring points from #01 to #05. Red line describes the normalized number of the Betti sequence and blue line denotes normalized u. The line is drawn at the position at α = 4.12 [deg] where transonic buffet was determined to have occurred with the naked eye from CFD animation.

series fluctuations are detected at #03 and #04.

Here we need to pay attention to the result of #03. This point is the most anterior position of the chordwise direction where the shockwave oscillation occurs. From the result of DES with fixed AoA, it was confirmed that shockwave oscillation begins at α 4.12 [deg], but this result shows the reaction at α 3.7288 [deg]. In the results of DES with fixed AoA, it was judged that the attack angle at which the shockwave started to oscillate was the occurrence of a transonic buffet, but in data mining using the Betti sequence, it is suggested that the transonic buffet already started at a lower angle of attack than α 4.12 [deg]. The invisible phenomenon is captured by the Betti sequence, which may be the temporal origination of the transonic buffet.

The time variation of the speed steadily appears at #05, but the value of the Betti sequence rises sharply to α of 3.6202

[deg]. Although no shockwave passes, it is suggested that an abnormal phenomenon occurs behind the shockwave. Due to a phenomenon earlier than α of 3.7288 [deg], which may be a sign of a transonic buffet at #03, the abnormal phenomenon that occurs behind the shockwave may be the beginning of a subsequent transonic buffet. Since we cannot completely deny the possibility that the transonic buffet is already occurring at α of 3.60 [deg], we need to use the sweep calculation result from the angle of attack of less than 3.60 [deg].

4. Feedback of Knowledge from Data Mining to Visualization

4.1. Observing Flow Structure at the Time Specified by Data Mining

We will observe the instantaneous flow structure at the specified time to construe the abnormality that PCP and the Betti sequence indicate. Figure 7 shows front upward visualization of C_p distribution on wing surface and iso-surface of $u = 0$ which describes flow separation boundary. This figure reveals that separation behavior has 3D non-linearity for spanwise direction.

A bird's-eye view is shown in Fig. 8 to clearly show the monitoring points around #5. Figure 8(a) shows that separation behind the shockwave is suppressed near $y = 0.10$. Separation does not grow and reattaches to the wing upper surface. According to Fig. 8(b), perturbation of C_p on the wing surface does not appear in the vicinity of #5, but there is a remarkable difference in the spatial structure of x-direction velocity u.

In contrast, as indicated by three arrows, we recognize a different tendency in Fig. 8(c) showing the viscosity distribution on the wing surface. These are the positions where the highly viscous region is maintained in the chordwise direction. That is, it can be confirmed that the three-dimensional nature of the flow structure with respect to the spanwise direction is generated. High viscosity elongation inhibits separation and causes reattachment. Differences between data indicated by PCP and abnormality indicated by the Betti sequence are due to instability in boundary layer transition.

The transonic buffet has three-dimensional structure in the spanwise, because shockwaves have three-dimensionality before reaching buffet. The three-dimensional nature of the shockwave arises from the twist of the average flow generated by the instability of the boundary layer transition on the wing surface. Since three-dimensionality exists regardless of whether transonic buffet occurs or not, instability due to boundary layer transition is probably not a direct cause of transonic buffet.

Consequently, Fig. 8 derived by PCP and the Betti Sequence suggests a physical mechanism to induce three-dimensionality in the spanwise direction. Since the difference of the physical quantity can capture the minute fluctuation, it succeeded in simply grasping the abnormality.

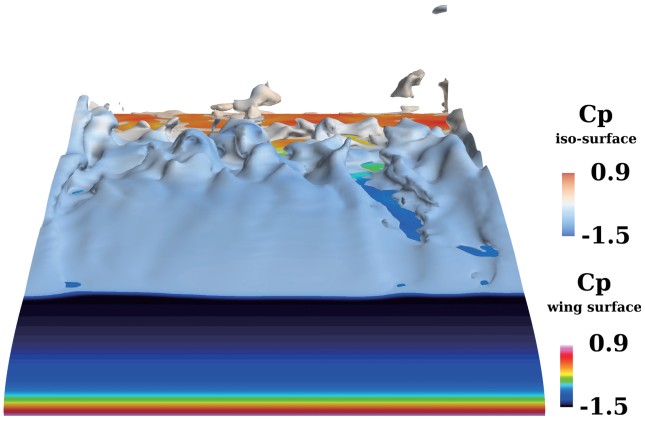

Fig. 7. Front upward visualization of the instantaneous flow structure at the time specified by data mining. Iso-surface of $u = 0$ and C_p distribution on the wing surface.

4.2. Hypothesis regarding Physical Mechanism of Transonic Buffet Outbreak

The consequences of data mining suggest the physical mechanism of transonic buffet as follows;

1. Shock is generated.
2. Pressure fluctuation is generated by shock. (*1)
3. The fluctuation propagates to upstream. (*2)
4. The fluctuation gives an effect on upstream velocity changes; upstream pressure also varies according to the

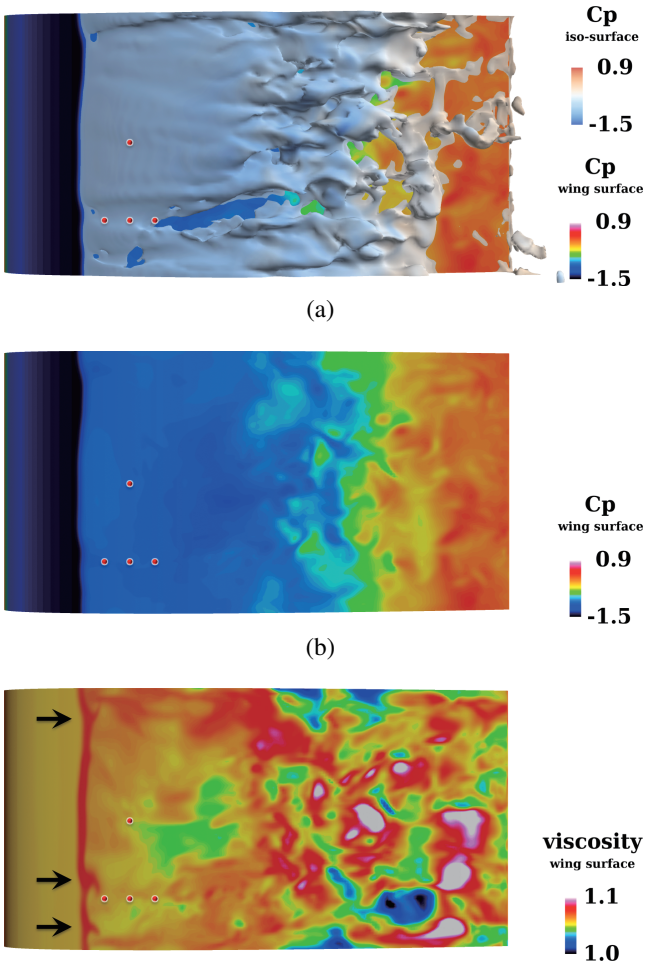

Fig. 8. Upward visualization of the instantaneous flow structure at the time specified by data mining. Red points represent the monitoring points #4, #5, #6, and #15. (a) Iso-surface of $u = 0$ and C_p distribution on the wing surface , (b) just C_p distribution on the wing surface, and (c) Laminar viscosity distribution on the wing surface. Red points denote the monitoring those.

following Rankine-Hugoniot relation:

$$\frac{\rho_2}{\rho_1} = \frac{u_1}{u_2} = \frac{1 + \dfrac{\gamma+1}{\gamma-1}\dfrac{p_2}{p_1}}{\dfrac{\gamma+1}{\gamma-1} + \dfrac{p_2}{p_1}}. \quad (2)$$

If u_1 decreases, p_1 increases. In contrast, if u_2 swells, p_1 declines.

5. Shock shifts to keep balance in the vicinity of it ? (*3)

To physically explain the above hypothesis, points of doubt are listed below:

- (*1) Why shock yields pressure fluctuation.
- (*2) How pressure fluctuation propagates to upstream. Where is the propagating path. If spatial propagation occurs, spatial monitoring points is necessary.
- (*3) What balance? Circulation?

Further data mining will be carried out to give a physical explanation to these in the future.

5. Conclusions

In this study, the data mining techniques such as from orthodox to state-of-the-art have been applied to the large scale unsteady aerodynamic data regarding transonic buffet generated by computational fluid dynamic analysis. As a result, several sign detection can be implemented. In response to this result, we have found that characteristic changes in the viscosity distribution of the wing surface can be seen as a result of visualizing the data around the time. Following the consequence, since we found the necessity of a more suitable dataset for examining the origination of a transonic buffet, further data mining will be performed for it, we will elucidate the physical mechanism of transonic buffet phenomenon. Design information obtained from data mining will lead to the geometry design that does not cause transonic buffet.

Acknowledgments

Part of this study was supported by Grant-in-Aid for Scientific Research (C) 16K00295, Japan Society for the Promotion of Science as well as the contract research JX-PSPC-44192 from JAXA. Whole images were created using FieldView16.1 as provided by Intelligent Light via its University Partners Program.

References

1) Lee, B. H. K., "Self-Sustained Shock Oscillations on Airfoils at Transonic Speeds," *Progress in Aerospace Sciences*, Vol. 37, 2001, pp. 147–196.
2) Hilton, W. F. and Fowler, R. G., "Photographs of Shock Wave Movement," National Physical Laboratories Report & Memoranda No. 2692.
3) Jacquin, L., Molton, P., Deck, S., Maury, B., and Soulevant, D., "Experimental Study of Shock Oscillation over a Transonic Supercritical Profile," *AIAA Journal*, Vol. 47, No. 9, 2009, pp. 1985–1994.
4) Fukushima, Y. and Kawai, S., "Wall-Modeled Large-Eddy Simulation of Transonic Buffet over a Supercritical Airfoil at High Reynolds Number," AIAA Paper 2017-0495, 2017.
5) Manyika, J., Chui, M., Brown, B., Bughin, J., Dobbs, R., Roxburgh, C., and Byers, A. H., *Big Data: The Next Frontier for Innovation, Competition, and Productivity*, Mckinsey Global Institute, 2011.
6) Hashimoto, A., Murakami, K., Aoyama, T., Ishiko, K., Hishida, M., Sakashita, M., and Lahur, P. R., "Toward the Fastest Unstructured CFD Code "FaSTAR"," AIAA Paper 2012-1075.
7) Obayashi, S. and Guruswamy, G. P., "Convergence Acceleration of an Aeroelastic Navier-Stokes Solver," *AIAA Journal*, Vol. 33, No. 6, 1994, pp. 1134–1141.
8) Spalart, P. R. and Allmaras, S. R., "A One-Equation Turbulence Model for Aerodynamic Flows," AIAA Paper 92-0439, 1992.
9) Sharov, D. and Nakahashi, K., "Reordering of Hybrid Unstructured Grids for Lower-Upper Symmetric Gauss-Seidel Computations," *AIAA Journal*, Vol. 36, No. 3, 1998, pp. 484–486.
10) Watanabe, S., Nakano, S., Chiba, K., and Kanazaki, M., "On-Demand Correlation-Based Information Hierarchical Structuring Method (CIHSM) for Non-Dominated Solutions," *Proceedings on IEEE World Congress on Computational Intelligence*, IEEE, 2016, pp. 1977–1984.
11) Inselberg, A., "The Plane with Parallel Coordinates," *The Visual Computer*, Vol. 1, No. 2, 1985, pp. 69–91.
12) Elmqvist, N., Dragicevic, P., and Fekete, J., "Rolling the Dice: Multidimensional Visual Exploration using Scatterplot Matrix Navigation," *IEEE Transactions on Visualization and Computer Graphics*, Vol. 14, No. 6, 2008, pp. 1539–1548.
13) van der Maaten, L., "Barnes-Hut-SNE," *CoRR*, Vol. abs/1301.3342, 2013.
14) Umeda, Y., "Time Series Classification via Topological Data Analysis," *Transactions of the Japanese Society for Artificial Intelligence*, Vol. 32, No. 3, 2017, pp. 1–12, D–G72.
15) Ali, S., Basharat, A., and Shah, M., "Chaotic Invariants for Human Action Recognition," *Proceedings on IEEE 11th International Conference on Computer Vision*, IEEE, Rio de Janeiro, Brazil, 2007, pp. 1–8.
16) Zomolodian, A. and Carlsson, G., "Computing Persistent Homology," *Discrete and Computational Geometry*, Vol. 33, No. 2, 2005, pp. 249–274.
17) Carlsson, G., "Topology and Data," *Bulletin of the American Mathematical Society*, Vol. 46, 2009, pp. 255–308.